

**Supplementary information (ESI)**

**A facile room temperature chemical transformation approach for binder-free thin film formation of Ag<sub>2</sub>Te and lithiation/delithiation chemistry of the film**

Eun-Kyung Kim<sup>a</sup>, Dasom Park<sup>b</sup>, Nabeen K. Shrestha<sup>a,\*</sup>, Jinho Chang<sup>b</sup>, Cheol-Woo Yi<sup>b</sup>, Sung-Hwan Han<sup>a,\*</sup>

---

<sup>a</sup>Institute of Materials Design, Department of Chemistry, Hanyang University, Seongdong-gu, 133791 Seoul, Republic of Korea.

E-mail: [nabeenkshrestha@hotmail.com](mailto:nabeenkshrestha@hotmail.com) (N.K. Shrestha); [shhan@hanyang.ac.kr](mailto:shhan@hanyang.ac.kr) (S.-H. Han).

<sup>b</sup>Department of Chemistry, Sungshin W. University, 55 Dobong-ro, 76ga-gil, Gangbuk-gu, Seoul 142-732, Republic of Korea.

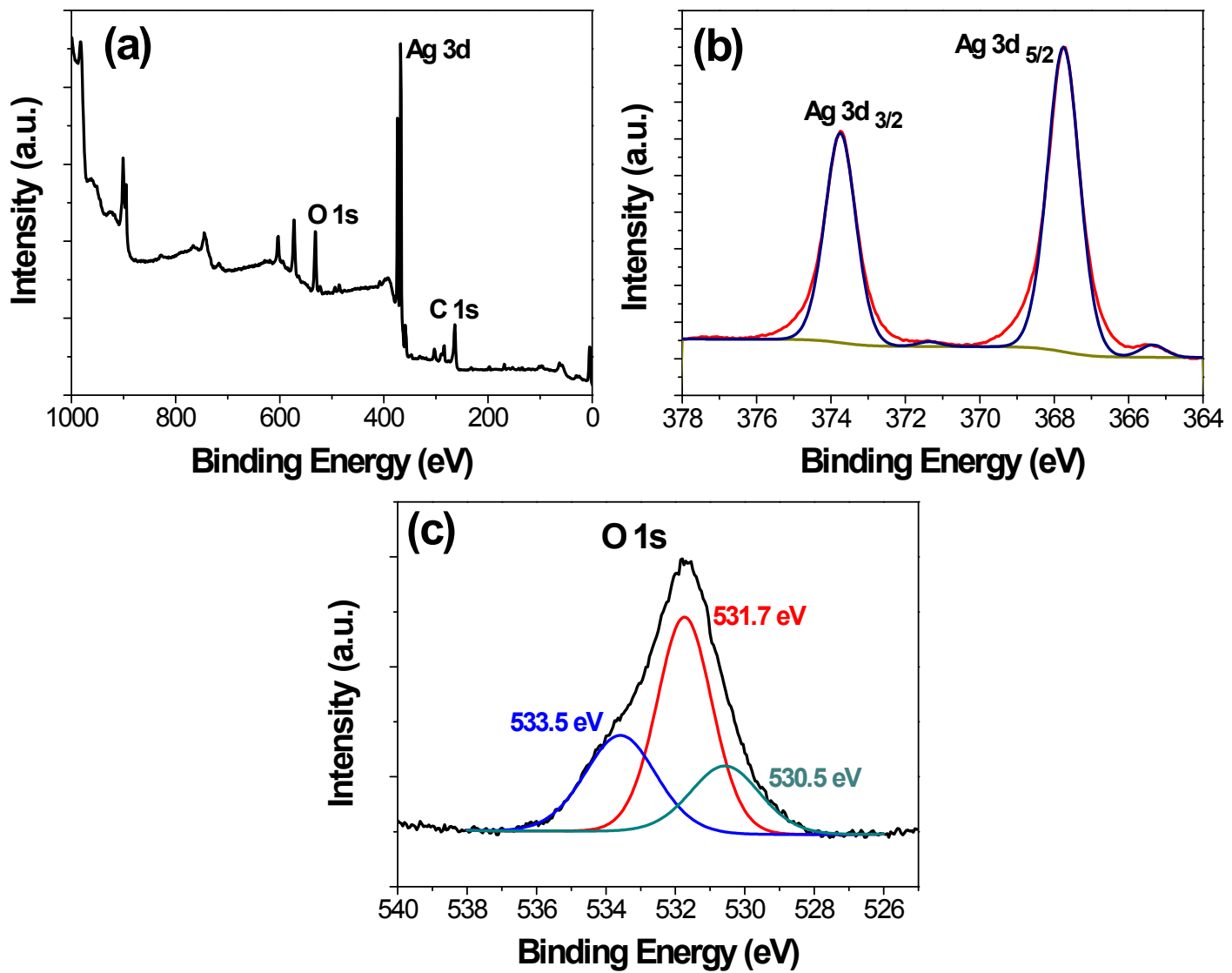


**Fig. S1.** XPS spectra of Ag/Ag<sub>x</sub>O film. (a) Survey spectrum, (b) Ag 3d core level spectrum, and (c) O 1s core level spectrum.

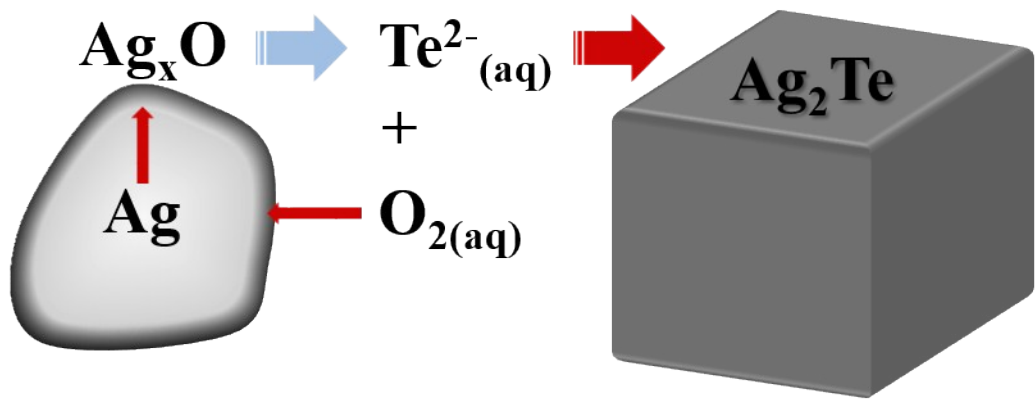


**Fig. S2.** Schematic diagram showing the surface oxidation of Ag particles followed by chemical transformation into  $\text{Ag}_2\text{Te}$  in presence of aqueous Te-precursor solution at room temperature.

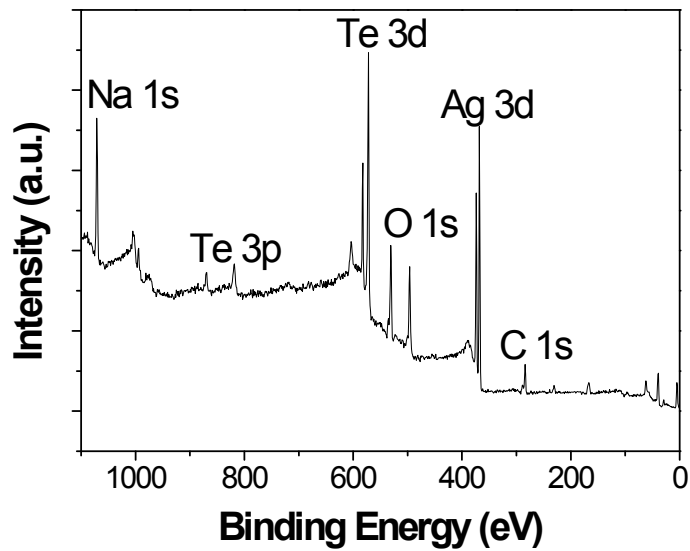


**Fig. S3.** XPS survey spectrum of chemically transformed  $\text{Ag}_2\text{Te}$  film. The Na signal at 1071.12 eV is attributed to residual  $\text{NaOH}$ .

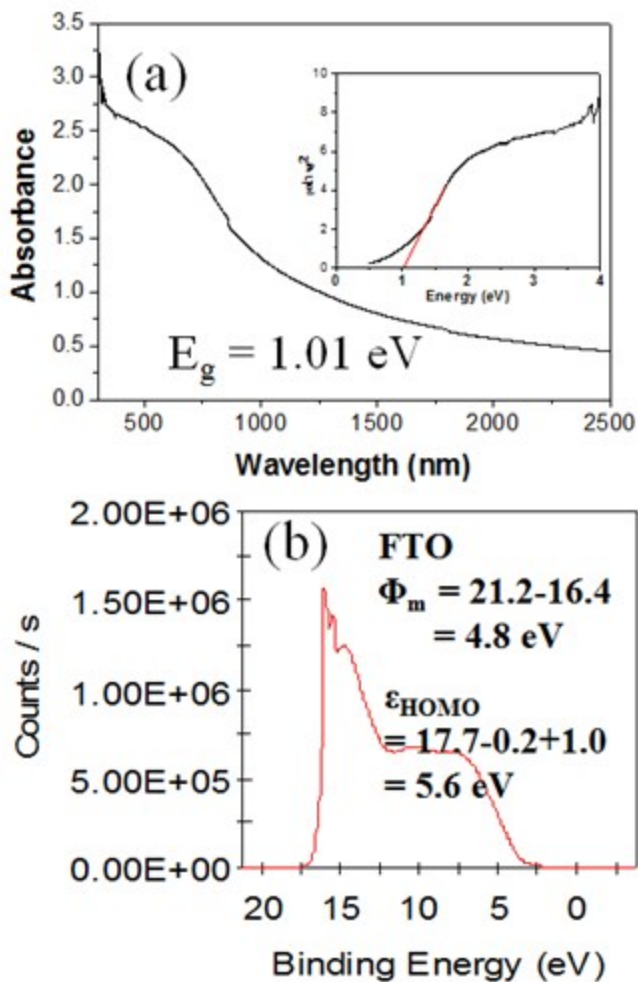


**Fig. S4.** (a) UV-vis absorption spectrum of  $\text{Ag}_2\text{Te}$  film and inset shows the Tauc plot for estimation of optical gap. (b) UPS spectrum for estimation of valance band edge position of  $\text{Ag}_2\text{Te}$  film. (c) Various parameters obtained from Hall measurement of the  $\text{Ag}_2\text{Te}$  film.

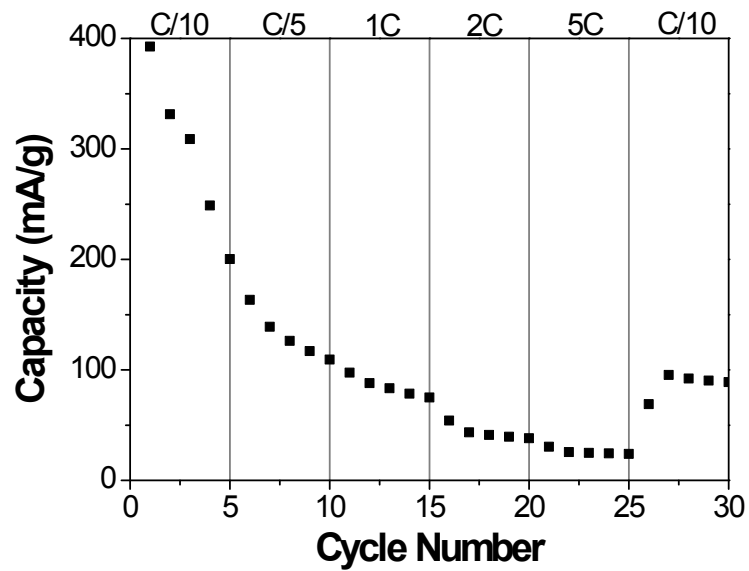


**Fig. S5** Charge–discharge curves of the Li/LiPF<sub>6</sub>/Ag<sub>2</sub>Te battery at various current densities.